Using Polyacrylamide Hydrogels to Model Physiological Aortic Stiffness Reveals that Microtubules Are Critical Regulators of Isolated Smooth Muscle Cell Morphology and Contractility

Sultan Ahmed[†], Robert. T. Johnson *[†], Reesha Solanki, Teclino Afewerki, Finn Wostear and Derek. T. Warren

School of Pharmacy, University of East Anglia, Norwich Research Park, Norwich, United Kingdom

Vascular smooth muscle cells (VSMCs) are the predominant cell type in the medial layer of the aortic wall and normally exist in a quiescent, contractile phenotype where actomyosin-derived contractile forces maintain vascular tone. However, VSMCs are not terminally differentiated and can dedifferentiate into a proliferative, synthetic phenotype. Actomyosin force generation is essential for the function of both phenotypes. Whilst much is already known about the mechanisms of VSMC actomyosin force generation, existing assays are either low throughput and time consuming, or qualitative and inconsistent. In this study, we use polyacrylamide hydrogels, tuned to mimic the physiological stiffness of the aortic wall, in a VSMC contractility assay. Isolated VSMC area decreases following stimulation with the contractile agonists angiotensin II or carbachol. Importantly, the angiotensin II induced reduction in cell area correlated with increased traction stress generation. Inhibition of actomyosin activity using blebbistatin or Y-27632 prevented angiotensin II mediated changes in VSMC morphology, suggesting that changes in VSMC morphology and actomyosin activity are core components of the contractile response. Furthermore, we show that microtubule stability is an essential regulator of isolated VSMC contractility. Treatment with either colchicine or paclitaxel uncoupled the morphological and/or traction stress responses of angiotensin II stimulated VSMCs. Our findings support the tensegrity model of cellular mechanics and we demonstrate that microtubules act to balance actomyosin-derived traction stress generation and regulate the morphological responses of VSMCs.

Keywords: actomyosin, contraction, matrix stiffness, microtubules, polyacrylamide hydrogel (PAH), traction force, vascular smooth muscle cell (VSMC)

INTRODUCTION

Vascular smooth muscle cells (VSMCs) are the predominant cell type in the medial layer of the arterial wall. VSMCs normally exist in a quiescent, contractile phenotype where actomyosin-derived contractile forces maintain vascular tone (Brozovich et al., 2016). However, VSMCs are not terminally differentiated and can down-regulate contractile markers and dedifferentiate into a proliferative, synthetic phenotype (Rzucidlo et al., 2007; Liu et al., 2015; Shi and Chen, 2016). Both

phenotypes retain the ability to generate actomyosin force that is essential for both VSMC contraction and migration (Ahmed and Warren, 2018; Afewerki et al., 2019). Contractile VSMCs possess a greater abundance of α-smooth muscle actin (αSMA) and smooth muscle-myosin heavy chain (SM-MyHC), that enhance their ability to generate actomyosin forces and contract (Rensen et al., 2007). However, both contractile and proliferative VSMCs generate actomyosin force via stimulating interactions between myosin II and filamentous actin. This process is regulated in both phenotypes by blood-borne factors, such as angiotensin II, that bind to receptors on the VSMC surface and mechanical factors including matrix stiffness and circumferential tension of the aortic wall (Qiu et al., 2010; Brozovich et al., 2016; Ahmed and Warren, 2018).

Young's modulus is a measure of material stiffness. Atomic force microscopy studies have determined that the Young's modulus of the medial layer of an elastic artery is between 5 and 37 kPa (Tracqui et al., 2011; Bae et al., 2016; Rezvani-Sharif et al., 2019). Microenvironment rigidity transmits 'outside-in' resistive forces to VSMCs and this process is dependent on focal adhesions that convey force between the extracellular matrix (ECM) and the cytoskeleton (Lacolley et al., 2017; Ahmed and Warren, 2018; Mohammed et al., 2019). VSMCs and other cell types respond to outside-in signals by exerting actomyosin based contractile forces on the matrix (inside-out forces) that scale with the outside-in resistive forces (Sun et al., 2008; Holle et al., 2018). Matrix rigidity rapidly activates Rho/ROCK signalling at ECM adhesions, initiating actin polymerisation and myosin light chain phosphorylation, thereby augmenting actomyosin activity (Ahmed and Warren, 2018). Actin cytoskeletal reorganisation and enhanced actomyosin activity increase VSMC integrated traction forces, the force VSMCs apply to the ECM (Li et al., 2020; Johnson et al., 2021). While much is known about VSMC actomyosin and contractile responses, we still lack an understanding of how VSMC structural and signalling components integrate to regulate these processes.

Extracellular mechanical forces, generated by the flow of blood and the mechanical properties of the ECM, programme the function of VSMCs (Johnson et al., 2021). In healthy arteries, VSMC contraction is initiated in response to blood pressure derived deformation of the arterial wall (Ye et al., 2014). However, these forces are not consistent and physiological cycle-by-cycle variations in blood pressure have been found to alter the contractile response of VSMCs (Bartolák-Suki et al., 2015; Bartolák-Suki and Suki, 2020). During ageing, the mechanical environment changes. Blood pressure increases, enhancing the compressional forces applied to the arterial wall; whilst the tensile strength and rigidity of the wall increases due to ECM remodelling (Tsamis et al., 2013). In response to these altered mechanical cues, VSMCs generate enhanced actomyosin derived contractile forces (Ye et al., 2014). This results in arterial stiffening, a hallmark of vascular ageing and cardiovascular disease onset (Glasser et al., 1997; Mitchell et al., 2010). How matrix stiffness induces enhanced VSMC actomyosin force production is unknown, but it is a response that is observed in many other cell types (Discher et al., 2005; Zhou et al., 2017; Pasqualini et al., 2018; Bastounis et al., 2019). It is therefore

imperative that studies investigating VSMC physiological force generation take this mechanical property into account. Traditionally, many *in vitro* experiments have cultured isolated VSMCs on plastic or glass, materials whose stiffness is around a thousand times greater than that of the arterial wall (Minaisah et al., 2016). More recently, the role of matrix stiffness in regulating VSMCs has been investigated using polyacrylamide hydrogels, a substrate whose stiffness can be tuned to a desired kPa. These studies have identified that matrix stiffness is a regulator of VSMC phenotype, with enhanced stiffness altering the proliferative, migratory and adhesive properties of VSMCs (Wong et al., 2003; Xie et al., 2018; Nagayama and Nishimiya, 2020; Rickel et al., 2020). Furthermore, matrix rigidity promoted actin cytoskeleton remodelling and stress fiber formation, increasing VSMC stiffness and traction stress generation (Brown et al., 2010; Sazonova et al., 2015; Petit et al., 2019; Sanyour et al., 2019). Whilst these studies controlled ECM rigidity, many of them made use of high passage VSMCs and culture conditions that would promote the synthetic phenotype. Therefore, the findings have little relevance for understanding VSMC contractile function.

Actomyosin derived contractile forces place stress and intracellular tension upon the cell. In other cell types, these deformational forces are proposed to be balanced by the ECM and the microtubule network (Johnson et al., 2021). This relationship is described by the tensegrity model, whereby microtubules act as compression bearing struts, capable of resisting strain generated by the actin cytoskeleton (Stamenović, 2005; Brangwynne et al., 2006). The balance between compression and strain defines cell shape and stability (Stamenović, 2005). This model predicts that microtubule destabilisation will increase actomyosin derived force generation. In support of this, treatment with microtubule destabilisers, such as colchicine, result in enhanced force generation within coronary and aortic vessels (Sheridan et al., 1996; Platts et al., 1999, 2002; Paul et al., 2000; Zhang et al., 2000). However, our understanding of the role of microtubules in VSMC contractile agonist responses remains limited and some data contradicts the tensegrity model. For example, wire myography showed that microtubule stabilisation had no effect on the ability of isolated aortic rings to contract (Zhang et al., 2000). Dynamic instability, the ability of microtubules to constantly cycle through phases of growth and shrinkage, is an inherent characteristic that enables the microtubule network to rapidly reorganise in response to the changing mechanical requirements of the cell (Nogales, 2001). Whilst observations regarding the function of microtubule stability in VSMC contraction have been made, our understanding of the mechanisms behind these observations remains incomplete.

One of the largest obstacles for identifying different mechanisms of VSMC contraction remains the lack of *in vitro* tools. The current gold standard for assessing isolated cell actomyosin activity is traction force microscopy (TFM) (Muhamed et al., 2017). TFM is used to quantitatively measure the stress exerted by a cell on its substrate, which is then used as an indicator of cell contractility (Kraning-Rush et al.,

2012; Lekka et al., 2021). Additionally, atomic force microscopy (AFM) has been used to assess actomyosin cortical tension and the force transduced through individual focal adhesion complexes (Sanyour et al., 2019). However, these techniques have several limitations, mainly being time consuming and low throughput (Haase and Pelling, 2015; Colin-York and Fritzsche, 2018; Schierbaum et al., 2019). Collagen gel assays, that are easily performed with generic lab equipment and skills, provide an alternative to these techniques. Typical collagen assays involve the suspension of a cell population in a prefabricated collagen gel. Contraction is then assessed by observing dimensional changes of the gel (Ngo et al., 2006). Limitations of collagen gels primarily relate to the qualitative nature of the assay and inconsistencies in gel shape. Collagen gels also lack rigidity control and are softer than the physiological arterial wall. These limitations severely affect the reproducibility and reliability of such assays (Vernon and Gooden, 2002).

Previous studies have reported that isolated VSMCs display a reduction in cell area upon contractile agonist stimulation (Li et al., 1999; Wang et al., 2017; Halaidych et al., 2019). Suggesting that changes in VSMC morphology and actomyosin activity are important components of the VSMC contractile response. Given their limitations, existing *in vitro* VSMC contractility assays are not able to investigate these processes. In this study we develop and validate an approach for screening isolated VSMC contraction using cell area as a reporter. The assay uses polyacrylamide hydrogels that are easily fabricated and mimic the rigidity of the physiological elastic arterial wall (Minaisah et al., 2016; Porter et al., 2020). Moreover, we show that combined with TFM, this technique allows investigation into factors that regulate both VSMC morphology and traction stress generation. Finally, we identify microtubule stability as a key regulator of VSMC contractile responses.

MATERIALS AND METHODS

Polyacrylamide Hydrogel Preparation

Hydrogels were prepared as described previously (Minaisah et al., 2016). Briefly 30 mm coverslips were activated by treating with (3-Aminopropyl)triethoxysilane for 2 min, washed 3x in dH$_2$O and fixed in 0.5% glutaraldehyde for 40 min. Coverslips were subsequently washed 3x in dH$_2$O and left to air dry. The required volume of 12 kPa polyacrylamide hydrogel mix (7.5% acrylamide, 0.15% bis-acrylamide in water) was supplemented with 10% APS (1:100) and TEMED (1:1,000) before 50 µl of the solution was placed on a standard microscopy slide and covered by an activated coverslip. Once set, the fabricated 12 kPa hydrogel was removed, placed into a 6-well plate, washed 3x with dH$_2$O and crosslinked with sulfo-SANPAH (1:3,000) under UV illumination (365 nm). Finally, hydrogels were washed with PBS and functionalised with collagen I (0.1 mg/ml) for 10 min at room temperature. Hydrogel stiffness was previously confirmed using a JPK Nanowizard-3 atomic force microscope (Porter et al., 2020).

Vascular Smooth Muscle Cell Culture and Drug Treatments

Human adult aortic VSMCs (passage 3–10) were purchased from Cell Applications Inc. (354-05a). VSMCs were grown in growth media (Cell Applications Inc.), prior to being washed with Earle's Balanced Salt Solution (Thermo) and seeded in basal media (Cell Applications Inc.) onto 12 kPa hydrogels, 18 h prior to drug treatment. Standard VSMCs culture was performed as described previously (Ragnauth et al., 2010; Warren et al., 2015).

Quiescent VSMCs were stimulated with either angiotensin II (0.01–100 µM) (Merck) or carbachol (0.01–100 µM) (Merck) for 30 min. For all other drug treatments, quiescent VSMCs were pretreated with the stated dose for 30 min, prior to co-treatment with angiotensin II (10 µM) for an additional 30 min. Please see **Supplementary Table S1** for a list of compounds used in this study.

Immunofluorescence and VSMC Area/ Volume Analysis

Following treatment, cells were fixed in 4% paraformaldehyde (actin cytoskeleton) or ice-cold methanol (microtubules), permeabilised with 0.5% NP40 and blocked in 3% BSA/PBS. Targets were visualized using antibodies raised against lamin A/C (SAB4200236, Sigma), or α-tubulin (3873S, CST) in combination with a relevant Alexa Fluor 488 secondary antibody (A1101 or A1103, Thermo). F-actin was stained using Rhodamine Phalloidin (R145, Thermo). All images were captured at 20x (cell area/volume) or 40x (microtubule organization) magnification using either a Zeiss LSM510-META or a Zeiss LSM980-Airyscan confocal microscope. Cell area was measured using FIJI, open-source software (Schindelin et al., 2012), whilst cell volume was calculated using Volocity 6.3.

Cold-Stable Microtubule Stability Assay

The number of cold-stable microtubules per cell was determined as previous (Atkinson et al., 2018). Briefly, after treatment, cells were placed on ice for 15 min before being washed once with PBS and twice with PEM buffer (80 µM PIPES pH 6.8, 1 mM EGTA, 1 mM MgCl$_2$, 0.5% Triton X-100 and 25% (w/v) glycerol) for 3 min. Cells were then fixed for 20 min in ice-cold MeOH and prepared for staining as detailed above. Cell nuclei were identified using DAPI. Images were captured at 40x magnification using an Axioplan Epifluorescent microscope.

Traction Force Microscopy

For Traction Force Microscopy (TFM), VSMCs were seeded onto 12 kPa hydrogels containing 0.5 µm red fluorescent (580/605) FluoSpheres (1:1,000) (Invitrogen). Imaging was performed using a Zeiss Axio Observer live cell imaging system that captured 20x magnification images every 2 min. TFM was performed either in real-time or as an end point assay whereby images were captured before and after cell lysis. Lysis was achieved by the addition of 0.5% Triton X-100. Drift was corrected using the ImageJ StackReg plugin and traction force was calculated using the ImageJ plugin described previously to measure FluoSphere displacement (Tseng
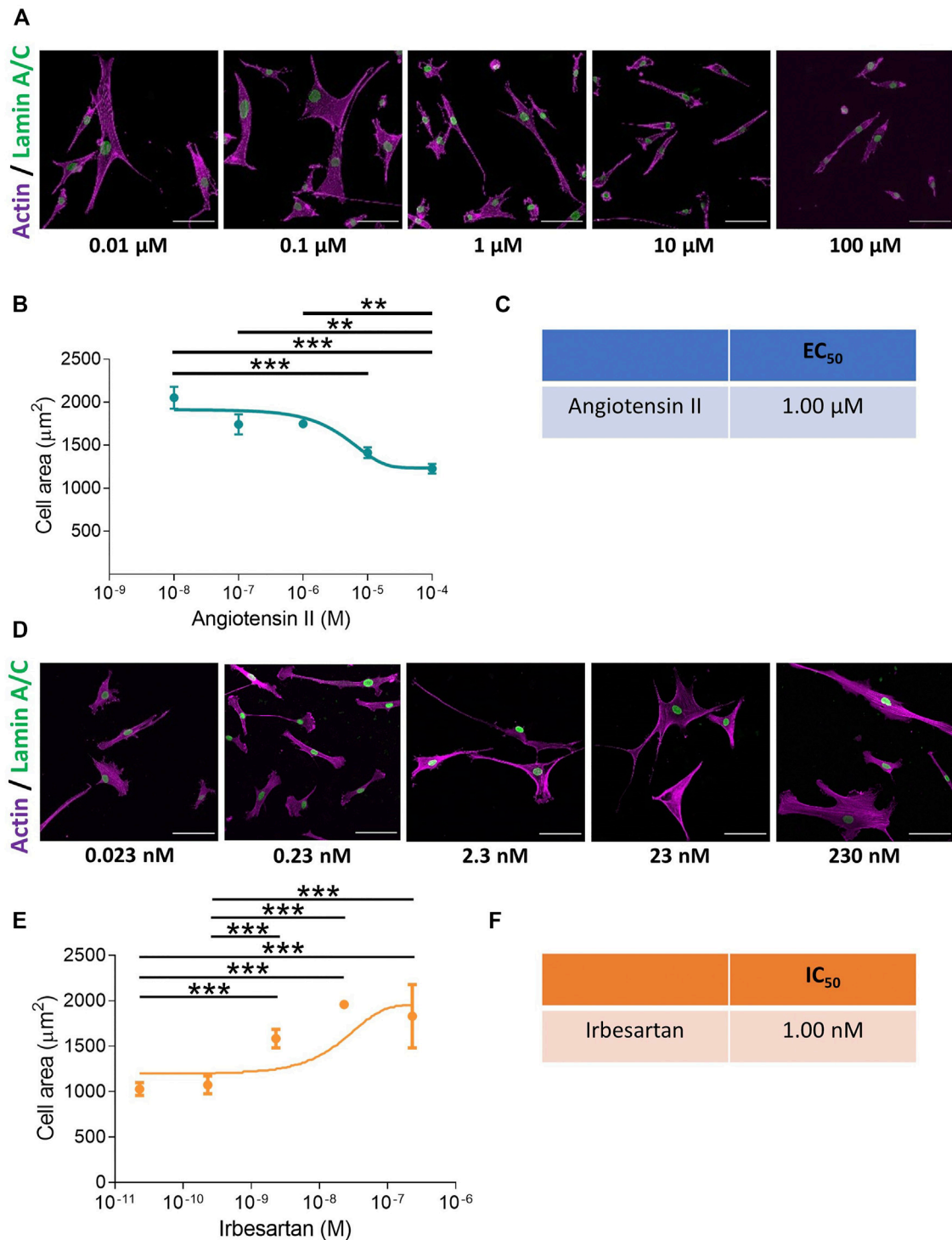
FIGURE 1 | VSMCs grown on pliable hydrogels display decreased area upon stimulation with the contractile agonist angiotensin II. **(A)** Representative images of isolated VSMCs cultured on 12 kPa polyacrylamide hydrogels treated with a range of angiotensin II concentrations for 30 min. Actin cytoskeleton (purple) and Lamin A/C labelled nuclei (green). Scale bar = 100 μm. **(B)** Isolated VSMC area, representative of 3 independent experiments with ≥150 cells analysed per condition. **(C)** EC_{50} of angiotensin II calculated from **(B)**. **(D)** Representative images of isolated VSMCs cultured on 12 kPa hydrogels and treated with angiotensin II (10 μM) for 30 min in the presence of a range of irbesartan concentrations. Actin cytoskeleton (purple) and Lamin A/C (green). Scale bar = 100 μm. **(E)** Isolated VSMC area, representative of 3 independent experiments with ≥50 cells analysed per condition. **(F)** IC_{50} of irbesartan calculated from **(E)**. (** = $p < 0.01$), (*** = $p < 0.001$).

et al., 2012). Briefly, bead displacement was measured using the first and last image of the movie sequence. The cell region was segmented by overlaying the traction map with the cell image, highlighting the cell traction region with an ROI and extracting the traction forces in each pixel by using the save XY coordinate function in FIJI (Porter et al., 2020).

Cell Viability Assay

Cell viability was determined using a RealTime-Glo™ MT Cell Viability Assay following manufacturers instruction. Briefly, 5,000 cells per well in a 96-well plate were exposed to a range of drug concentrations for 1 h, prior to luminescence being measured using a Wallac EnVision 2,103 Multilabel Reader (PerkinElmer).

Statistics

All statistical analyses were performed in GraphPad Prism 6.05. Dose response curves are presented as the mean data ± SEM (error bars) plotted on a logarithmic dose response scale. EC_{50} and IC_{50} data were generated by non-linear regression. Results are presented as mean ± SEM. Dot plot graphs are presented to show data distribution, with each point corresponding to an individual cell measurement. Bars indicate the mean value, ± SEM (error bars). Comparison of multiple groups was achieved using a one-way ANOVA analysis with Bonferroni post-hoc test. For comparison of two groups, unpaired student t-tests were performed. Analysis of the real time Angiotensin II contraction data was performed using non-linear regression. A one phase association analysis was performed on traction stress vs time data and a one phase decay analysis was performed on the VSMC area vs time data.

RESULTS

Contractile Agonist Stimulation Reduces VSMC Area on Pliable Hydrogels

We set out to develop a screen, performed at a physiologically relevant rigidity, to unravel mechanisms regulating VSMC actomyosin activity and contraction (**Supplementary Figure S1**). Quiescent VSMCs grown on pliable, 12 kPa hydrogels were treated with a concentration range of the contractile agonists, angiotensin II or carbachol. Contractile response was measured through changes in VSMC area, which previous studies have shown correlates with isolated VSMC contractile activity (Li et al., 1999; Wang et al., 2017; Halaidych et al., 2019). Analysis confirmed that contractile agonist stimulation resulted in a reduction in VSMC area (**Figures 1A,B** and **Supplementary Figures S2A,B**). Further analysis of VSMC area revealed the assay could be used to determine the EC_{50} values of both angiotensin II and carbachol (**Figure 1C** and **Supplementary Figures S2C**), confirming the assay could be used to measure and compare agonist potency. Subsequent experiments were performed with 10 μM angiotensin II, a dose that produced the maximal response (**Figures 1A,B**). To observe the effect of angiotensin II stimulation on isolated VSMC volume, we next performed confocal microscopy. Analysis revealed that angiotensin II stimulated VSMCs displayed a reduction in area, but no change in volume (**Supplementary Figure S3**).

To confirm that the change in area was specific for receptor activation, we utilised the angiotensin II antagonist irbesartan and the cholinergic antagonist, atropine. VSMCs grown on pliable hydrogels were stimulated with angiotensin II or carbachol in the presence of an increasing dose of irbesartan or atropine, respectively. As expected, irbesartan and atropine treatment prevented a reduction in VSMC area, confirming that these changes were driven by receptor activation (**Figures 1D–F** and **Supplementary Figure S4**).

Myosin II Mediated Traction Stress Drives Changes in Angiotensin II Stimulated VSMC Area

The above data demonstrated the validity of our approach in generating EC_{50} and IC_{50} data for agonists/antagonists of isolated VSMC contractile function. We next sought to confirm that changes in VSMC area were due to contraction and not due to membrane retraction. To do this, we performed traction force microscopy to measure the displacement of beads embedded within the hydrogels. Analysis revealed that angiotensin II treatment stimulated VSMCs to contract, with a significant reduction in cell area observed after 8 min (**Figures 2A,B**). Importantly, beads moved towards VSMCs and both maximal and integrated traction stress increased rapidly and plateaued after 8 min (**Figures 2A,C,D**). This data confirmed the correlation between reduced VSMC area and traction stress generation upon angiotensin II stimulation. To further confirm that actomyosin derived force was driving these changes in VSMC area, we next used the myosin II inhibitor blebbistatin and the ROCK inhibitor Y-27632. As expected, treatment with either blebbistatin or Y-27632 blocked the angiotensin II mediated reduction in area, however, actomyosin inhibited VSMCs possessed an increased volume, compared to their angiotensin II treated counterparts (**Figure 3**). This confirmed that actomyosin activation was driving VSMC contraction in our system.

Microtubule Destabilisation Alters the Morphological Response of Angiotensin II Stimulated VSMCs

Microtubule depolymerisation increases the constriction and myogenic tone of aortic and carotid tissues (Leite and Webb, 1998; Platts et al., 2002; Johnson et al., 2021). However, the precise impact of microtubule disruption on VSMC contraction remains unknown. To address this, we determined the impact of angiotensin II stimulated VSMC contraction upon microtubule organisation and stability. Angiotensin II stimulation promoted the microtubule network to reorganise, switching from a straight, elongated arrangement of parallel microtubules to a more interlinking meshwork of microtubules (**Supplementary Figure S5**). Although angiotensin II stimulation induced the reorganisation of the microtubule cytoskeleton, there was no change in the number of cold-stable microtubules between
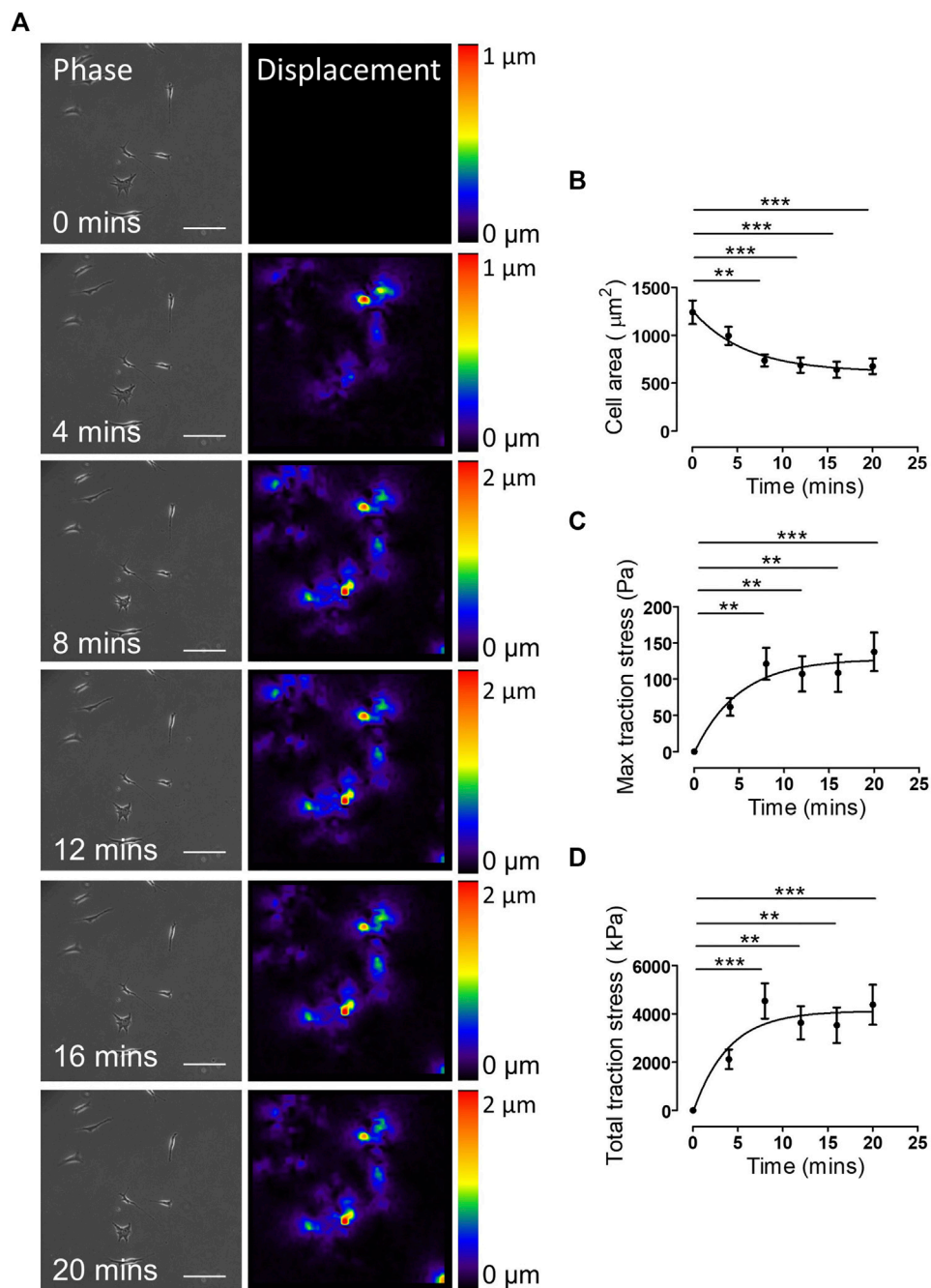
FIGURE 2 | Traction stress generation correlates with decreased VSMC area following angiotensin II stimulation. **(A)** Representative phase images and bead displacement heat maps of isolated VSMCs grown on 12 kPa polyacrylamide hydrogels and stimulated with angiotensin II over a 20 min time course. Scale bar = 100 μm. Displacement heat maps were generated by comparing the bead displacement for each time point to their initial positions at $t = 0$, as such there is no displacement at $t = 0$. **(B)** Isolated VSMC area, **(C)** maximum traction stress and **(D)** total traction stress generated at each time point compared to $t = 0$. Graphs represent the combined data from 3 independent experiments, with measurements taken from 35 VSMCs. (** = $p < 0.01$), (*** = $p < 0.001$).

quiescent and angiotensin II stimulated VSMCs (**Figures 4A,B**). Next, we used our assay to test the impact of microtubule disruption on VSMC contraction. Colchicine, a microtubule destabiliser, induced a concentration dependent increase in angiotensin II treated VSMC area, suggesting that microtubule depolymerisation was promoting VSMC relaxation (**Figures 4C–E**). In contrast, paclitaxel, a microtubule stabiliser, had no effect on the area of angiotensin II treated VSMCs (**Figures 4F,G**). Analysis confirmed that the concentrations of colchicine or paclitaxel used were sufficient to reduce or increase the number of cold-stable microtubules respectively (**Supplementary Figures S6A–D**). Furthermore, these concentrations produced no
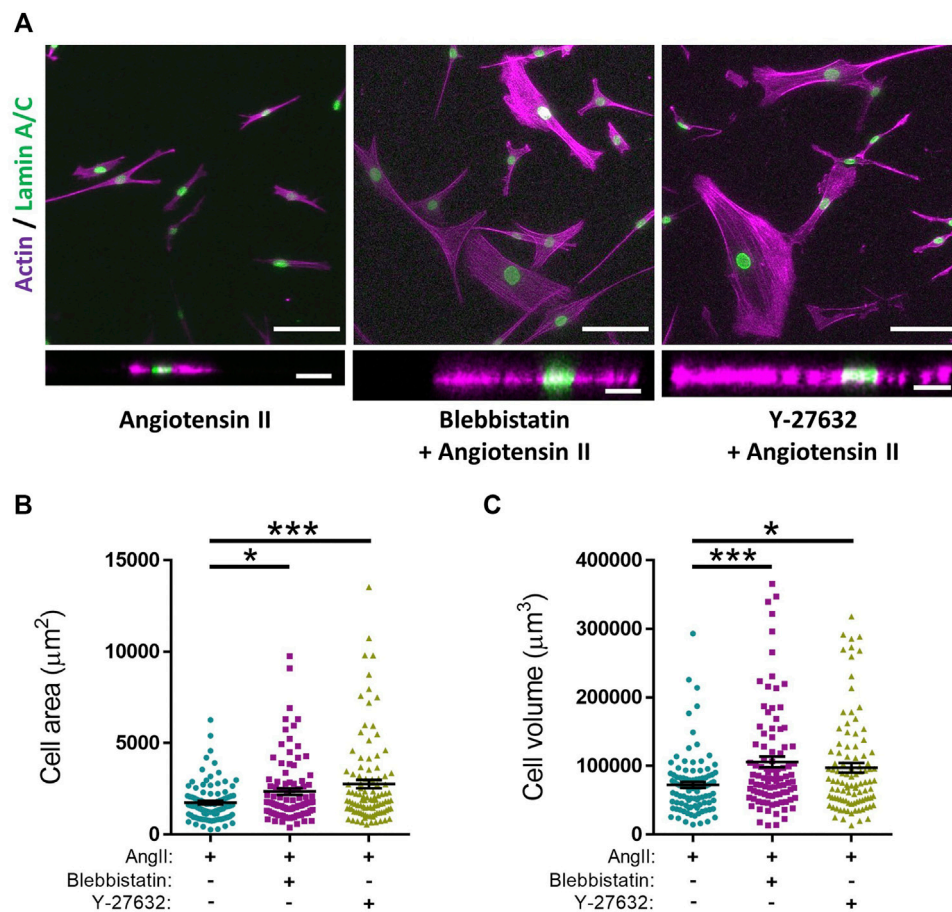
FIGURE 3 | Actomyosin inhibition prevents angiotensin II induced changes in VSMC area and increases VSMC volume on pliable hydrogels. **(A)** Representative images of isolated VSMCs cultured on 12 kPa polyacrylamide hydrogels pre-treated with either blebbistatin or Y-27632 for 30 min prior to cotreatment with angiotensin II (AngII) (10 µM) for an additional 30 min. Actin cytoskeleton (Rhodamine phalloidin, Purple) and Lamin A/C (green). Top—Representative XY images of VSMC area. Scale bar = 100 µm. Bottom—Representative XZ images of VSMC height. Scale bar = 30 µm. **(B)** Isolated VSMC area and **(C)** Isolated VSMC volume. Both **(B,C)** are representative of 3 independent experiments with ≥95 cell analysed per condition. (* = $p < 0.05$), (*** = $p < 0.001$).

significant reductions in cell viability (**Supplementary Figures S6E,F**). Surprisingly, confocal microscopy revealed that colchicine increased VSMC volume (**Figures 5A–C**), whereas the volume of paclitaxel treated VSMCs remained unchanged (**Figure 5D–F**).

Changes in Microtubule Stability Alters the Traction Stress Generation of Isolated VSMCs

The data above suggested that microtubule destabilisation was altering the angiotensin II induced area/volume response of isolated VSMCs. Previous studies using wire or pressure myography have reported that microtubule destabilisation increased VSMC force generation (Paul et al., 2000; Zhang et al., 2000; Platts et al., 2002). To confirm the impact of microtubule destabilisation on actomyosin activity, TFM was performed to measure traction stresses exerted by VSMCs. In agreement with previous studies, analysis revealed that pre-treatment with colchicine increased the maximal and total

traction stress exerted by angiotensin II stimulated VSMCs (**Figures 6A–C**). Finally, we examined the effect of microtubule stabilisation on traction stress. Paclitaxel pre-treatment had no effect on maximal traction stress. However, total traction stress was reduced when compared to their untreated counterparts (**Figures 6D–F**). This confirmed that maintenance of microtubule dynamics was essential for VSMC actomyosin activity and force generation.

DISCUSSION

Whilst much is known about VSMC contractile responses in physiology, *in vitro* assays to examine this process remain limited. Tissue culture plastic and glass are approximately a thousand times stiffer than the aortic wall (Minaisah et al., 2016), meaning that changes in VSMC area are driven by membrane retraction rather than contraction. Existing technologies to examine the contractile response of isolated VSMCs are either low throughput, such as TFM, or are
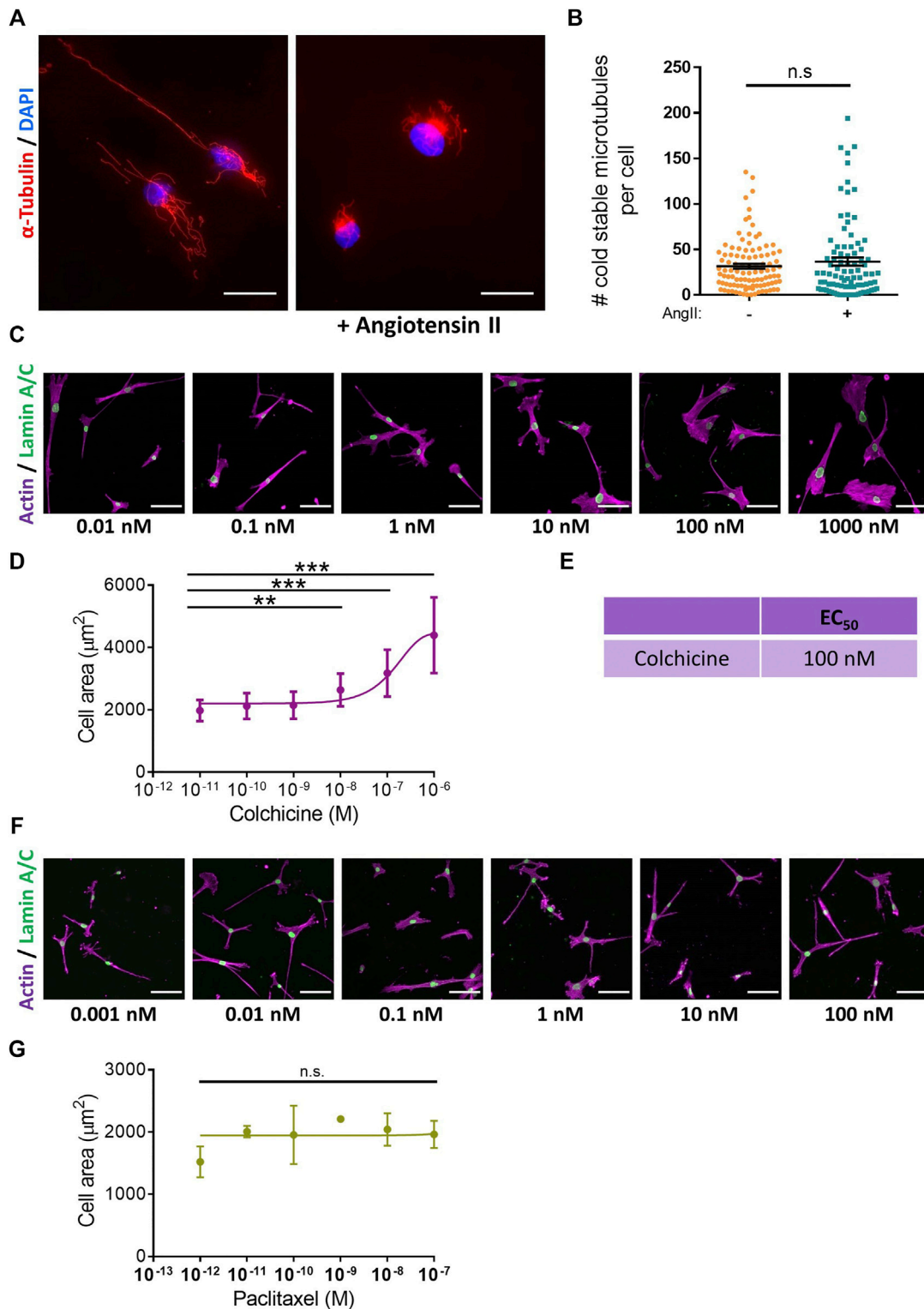
FIGURE 4 | Microtubule destabilisation prevents angiotensin II induced changes in VSMC area. **(A)** Representative images of isolated VSMCs cultured on 12 kPa polyacrylamide hydrogels, stained for cold-stable microtubules (α-tubulin, red) and cell nuclei (DAPI, blue). Scale bar = 50 µm. Angiotensin II (AngII) (10 µM) stimulation was performed for 30 min. **(B)** Number of cold-stable microtubules per cell, representative of 4 independent experiments, with ≥90 cells analysed per condition. **(C)** Representative images of isolated VSMCs cultured on 12 kPa hydrogels pre-treated with a range of colchicine concentrations for 30 min prior to cotreatment with angiotensin II (10 µM) for an additional 30 min. Actin cytoskeleton (purple) and Lamin A/C (green). Scale bar = 100 µm. **(D)** Isolated VSMC area, representative of 3

(Continued)

FIGURE 4 | independent experiments with ≥55 cells analysed per condition. **(E)** EC_{50} of colchicine calculated from **(D)**. **(F)** Representative images of isolated VSMCs cultured on 12 kPa hydrogels pre-treated with a range of paclitaxel concentrations for 30 min prior to cotreatment with angiotensin II (10 μM) for an additional 30 min. Actin cytoskeleton (purple) and Lamin A/C (green). Scale bar = 100 μm. **(G)** Isolated VSMC area, representative of 3 independent experiments with ≥65 cells analysed per condition. (n.s. = non-significant), (** = $p < 0.01$), (*** = $p < 0.001$).
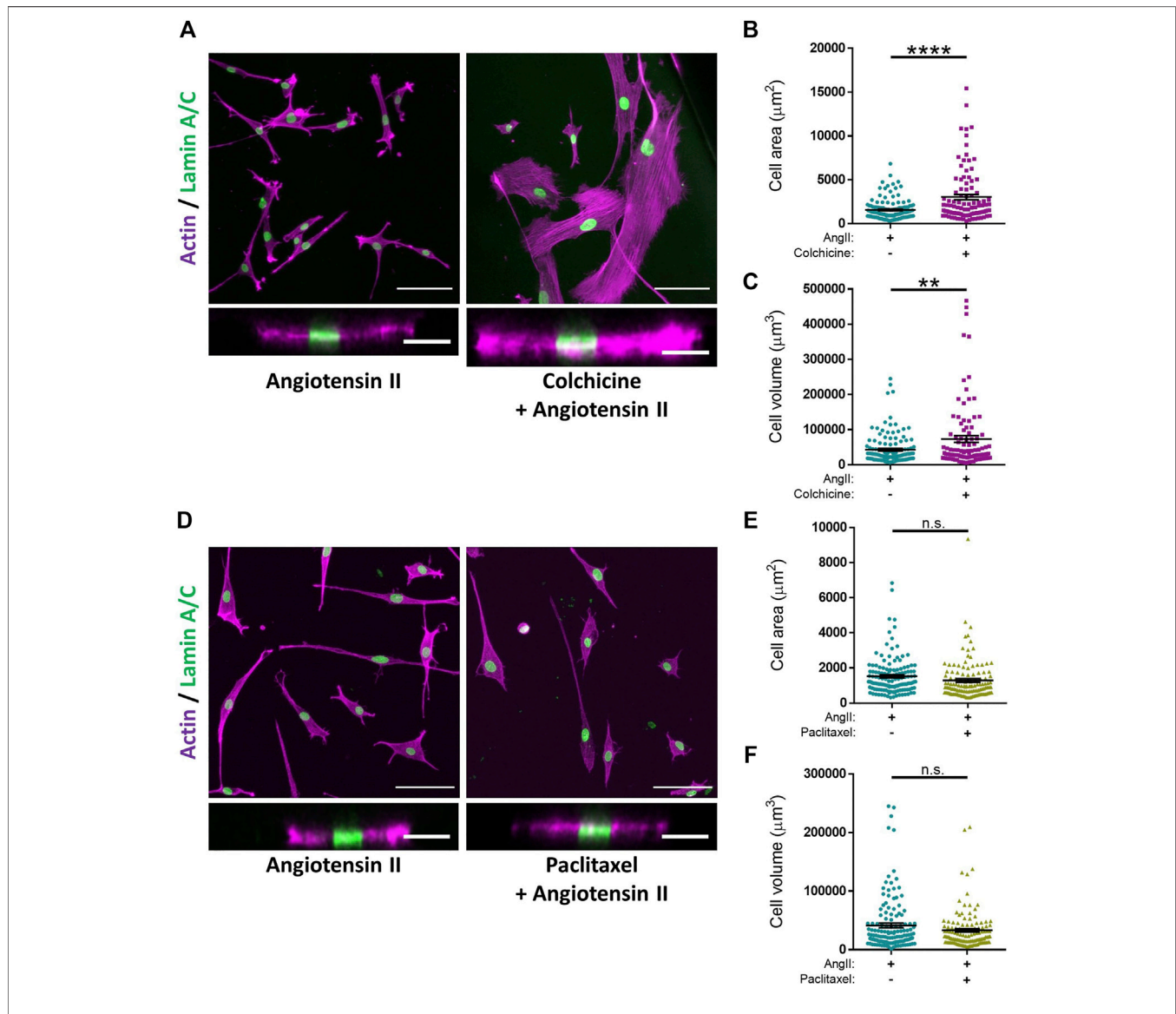
FIGURE 5 | Microtubule destabilisation alters angiotensin II stimulated VSMC volume on pliable hydrogels. **(A)** Representative images of isolated VSMCs cultured on 12 kPa polyacrylamide hydrogels pre-treated +/− colchicine (100 nM) for 30 min prior to cotreatment with angiotensin II (AngII) (10 μM) for an additional 30 min. Actin cytoskeleton (purple) and Lamin A/C (green). Top—Representative XY images of VSMC area. Scale bar = 100 μm. Bottom—Representative XZ images of VSMC height. Scale bar = 30 μm. **(B)** Isolated VSMC area and **(C)** Isolated VSMC volume. Both **B&C** are representative of 3 independent experiments with ≥100 cell analysed per condition. **(D)** Representative images of isolated VSMCs cultured on 12 kPa polyacrylamide hydrogels pre-treated +/− paclitaxel (1 nM) for 30 min prior to cotreatment with angiotensin II (AngII) (10 μM) for an additional 30 min. Actin cytoskeleton (purple) and Lamin A/C (green). Top—Representative XY images of VSMC area. Scale bar = 100 μm. Bottom—Representative XZ images of VSMC height. Scale bar = 30 μm. **(E)** Isolated VSMC area and **(F)** Isolated VSMC volume. Both **(E,F)** are representative of 3 independent experiments with ≥125 cell analysed per condition. (n.s. = non-significant), (** = $p < 0.01$), (**** = $p < 0.0001$).

inconsistent and lack rigidity control, such as the collagen gel assay (Vernon and Gooden, 2002; Colin-York and Fritzsche, 2018). We therefore set out to establish and validate a polyacrylamide hydrogel-based assay for screening the contractility of isolated VSMCs. Polyacrylamide hydrogels are widely used in cell biology and can be easily fabricated with generic research equipment and skills (Kandow et al., 2007; Caliari and Burdick, 2016; Minaisah et al., 2016; Mohammed et al., 2019). To enable VSMC attachment,

FIGURE 6 | Microtubule stability regulates angiotensin II induced VSMC traction stress generation. **(A)** Representative phase images and bead displacement heat maps of isolated VSMCs grown on 12 kPa polyacrylamide hydrogels. Cells were pre-treated +/− colchicine (100 nM) for 30 min prior to cotreatment with angiotensin II (AngII) (10 μM) for an additional 30 min. Scale bar = 100 μm. **(B)** Maximum traction stress and **(C)** Total traction stress generation. Both **(B,C)** are representative of 3 independent experiments with ≥48 cell analysed per condition. **(D)** Representative phase images and bead displacement heat maps of isolated VSMCs grown on 12 kPa polyacrylamide hydrogels. Cells were pre-treated +/− paclitaxel (1 nM) for 30 min prior to cotreatment with angiotensin II (AngII) (10 μM) for an additional 30 min. Scale bar = 100 μm. **(E)** Maximum traction stress generation and **(F)** Total traction stress generation. Both **(E,F)** are representative of 3 independent experiments with ≥38 cell analysed per condition. (n.s. = non-significant), (** = $p < 0.01$), (*** = $p < 0.001$), (**** = $p < 0.0001$).

polyacrylamide hydrogels mimicking physiological rigidity must be functionalised by ECM components such as collagen, fibronectin or lamin (Brown et al., 2010; Sazonova et al., 2015). Previous studies have utilised hydrogels of varying stiffness to identify matrix rigidity as a key regulator of VSMC morphology, migration, proliferation and phenotype. In response to matrix stiffness, VSMCs downregulate the expression of contractile markers SM-MyHC, calponin and smoothelin, whilst increasing the expression of proliferative genes Cyclin A and PCNA (proliferating cell nuclear antigen), in correlation with increased VSMC proliferation (Brown et al., 2010; Sazonova et al., 2015; Xie et al., 2018; Nagayama and Nishimiya, 2020). Additionally, VSMCs

undergo durotaxis, preferentially migrating from soft to stiff matrix rigidity, although the effect of matrix stiffness on the rate of migration appears dependent on the ECM component (Wong et al., 2003; Rickel et al., 2020).

In our present study, we describe a novel assay in which agonist induced VSMC contraction is performed on a substrate of physiological stiffness. We demonstrate that changes in isolated VSMC area were driven by angiotensin II induced traction stress generation, that pulled the compliant hydrogels towards the VSMC, decreasing cell area (**Figures 1A,B, 2**). Demonstrating that, isolated VSMC area can be used as a reporter of contractility on pliable hydrogels. VSMC volume remained unchanged by

contractile agonist stimulation (**Supplementary Figure S3**). Importantly, this assay was sensitive enough to generate EC_{50} and IC_{50} information of contractile agonists and antagonists, respectively (**Figures 1C,F**; **Supplementary Figures S2C, S4C**. Whilst TFM alone can measure the contractile response of VSMCs, it requires a large number of individual cells to be analysed in order to achieve consistent results (Petit et al., 2019). Through using cell area as a marker of VSMC contractility, a concentration range of potential agonists/ antagonists can be rapidly trialed, identifying the efficacy and optimal dose of a compound. Changes in VSMC area can subsequently be correlated to altered traction force generation using TFM in a targeted approach. We also predict that our assay could easily be used in conjunction with siRNA mediated depletion or overexpression strategies. Immunofluorescent co-staining, using antibodies against the targeted protein, would ensure only depleted or overexpressing cells are analysed. Therefore, this assay possesses the flexibility to enable the precise interrogation of complex biological pathways that regulate VSMC contractile function.

We have used this polyacrylamide hydrogel-based assay to investigate the role of microtubule stability in isolated VSMC morphology and traction stress generation. We identify microtubule stability as a critical regulator of isolated VSMC contractility and show that proper microtubule stability is essential to couple VSMC morphology and traction stress generation (**Figures 4C–G**, **6**). Our findings fit the tensegrity model of cellular mechanics (Stamenović, 2005); microtubule destabilisation increased traction stress generation, whereas microtubule stabilisation had the opposite effect (**Figure 6**). Our findings are supported by previous studies that show microtubule destabilising agents promoted an increase in isometric force generation by wire myography (Sheridan et al., 1996; Platts et al., 1999, 2002; Paul et al., 2000; Zhang et al., 2000). Whilst overall microtubule stability is maintained (**Figures 4A,B**), angiotensin II induced contraction initiates remodelling of the microtubule network (**Supplementary Figure S5**). Further work is required to understand the importance of this reorganisation, however, a recent study has demonstrated that stretched-induced reorganisation of VSMC microtubules enhances the efficiency of mitochondrial ATP production, thereby increasing actomyosin force generation (Bartolák-Suki et al., 2015).

However, contradictory to our findings (**Figures 6D–F**), previous studies have shown that microtubule stabilisation does not alter VSMC force generation by wire myography (Zhang et al., 2000). In this study, we show that paclitaxel had no effect on VSMC morphology (**Figures 4F,G**) and this may potentially account for this discrepancy. Additionally, we identify the IC_{50} of colchicine to be within the nanomolar range (**Figures 4C–E**). Paclitaxel also demonstrated significant microtubule stabilisation when used in the nanomolar range (**Supplementary Figures S6C,D**). However, previous studies have used microtubule targeting agents in the tens of micromolar range (Platts et al., 1999; Paul et al., 2000; Zhang et al., 2000). Numerous studies have shown that these agents can be cytotoxic in micromolar and, in some cell lines, nanomolar ranges (Pasquier et al., 2006; Thomopoulou et al., 2016; Atkinson et al., 2018; Abbassi et al.,

2019; Čermák et al., 2020). Meanwhile, in the present study we used these agents in nanomolar ranges, which had no effect on VSMC viability (**Supplementary Figures S6E,F**). Surprisingly, wire myography has shown that VSMC death does not trigger a reduction in isometric force generation (Clarke et al., 2006). Previously, a tamoxifen model that induced VSMC death resulted in the loss of approximately two thirds of VSMCs. However, the remaining VSMCs generated more contractile forces, resulting in the maintenance of the overall isometric force generation (Clarke et al., 2006). This observation may account for the divergence from the tensegrity model predictions, as seen in previous studies (Zhang et al., 2000). Clearly more research is needed to clarify the role of microtubules and cell death in regulating VSMC contractility and vascular tone.

As described above, our microtubule stabilisation/ destabilisation traction stress data fits the tensegrity model of cellular mechanics (**Figure 6**). However, we also show that microtubule destabilisation/stabilisation uncoupled the morphological response from the amount of traction stress VSMCs generated following angiotensin II stimulation (**Figure 5**). In our assay, isolated VSMC volume was unchanged by contractile agonist stimulation and changes in area were driven by actomyosin induced contraction (**Supplementary Figures S2, S3**). Microtubule destabilisation promoted increased VSMC volume (**Figures 5A,C**), and we propose that this increased volume is enhancing spreading in these cells. We predicted that these cells were undergoing a hypertrophic response, however more work is needed to clarify how these cells respond over a longer time course. Surprisingly, inhibition of non-muscle myosin II or ROCK also resulted in enhanced VSMC volume (**Figures 3A,C**). This suggests that actin and microtubule networks may mechanically cooperate to regulate VSMC volume control. Much is known about the synergistic nature of microtubules and actomyosin activity. Indeed, non-muscle myosin II has been shown to suppress microtubule growth in order to stabilise cell morphology (Sato et al., 2020), whilst microtubule acetylation has been found to regulate actomyosin-derived force generation (Joo and Yamada, 2014; Seetharaman et al., 2021). Actomyosin and microtubule cross-talk also regulates morphology during differentiation and cell migration in a variety of cell types (Akhshi et al., 2014; Wu and Bezanilla, 2018; Seetharaman and Etienne-Manneville, 2020), suggesting that communication between these mechanical networks is fundamentally important in determining VSMC morphology.

DATA AVAILABILITY STATEMENT

The raw data supporting the conclusion of this article will be made available by the authors, without undue reservation.

AUTHOR CONTRIBUTIONS

SA, RJ, RS, TA, and FW were responsible for performing experiments and analysed data. DW analysed data. RJ and

SUPPLEMENTARY MATERIAL

The Supplementary Material for this article can be found online at: https://www.frontiersin.org/articles/10.3389/fphar.2022.836710/full#supplementary-material

REFERENCES

Abbassi, R. H., Recasens, A., Indurthi, D. C., Johns, T. G., Stringer, B. W., Day, B. W., et al. (2019). Lower Tubulin Expression in Glioblastoma Stem Cells Attenuates Efficacy of Microtubule-Targeting Agents. *ACS Pharmacol. Transl. Sci.* 2, 402–413. doi:10.1021/acsptsci.9b00045

Afewerki, T., Ahmed, S., and Warren, D. (2019). Emerging Regulators of Vascular Smooth Muscle Cell Migration. *J. Muscle Res. Cel Motil* 40, 185–196. doi:10.1007/s10974-019-09531-z

Ahmed, S., and Warren, D. T. (2018). Vascular Smooth Muscle Cell Contractile Function and Mechanotransduction. *Vp* 2, 36. doi:10.20517/2574-1209.2018.51

Akhshi, T. K., Wernike, D., and Piekny, A. (2014). Microtubules and Actin Crosstalk in Cell Migration and Division. *Cytoskeleton (Hoboken)* 71, 1–23. doi:10.1002/cm.21150

Atkinson, S. J., Gontarczyk, A. M., Alghamdi, A. A., Ellison, T. S., Johnson, R. T., Fowler, W. J., et al. (2018). The β3-integrin Endothelial Adhesome Regulates Microtubule-dependent Cell Migration. *EMBO Rep.* 19, 1. doi:10.15252/embr.201744578

Bae, Y. H., Liu, S. L., Byfield, F. J., Janmey, P. A., and Assoian, R. K. (2016). Measuring the Stiffness of *Ex Vivo* Mouse Aortas Using Atomic Force Microscopy. *J. Vis. Exp.* 54630, 1. doi:10.3791/54630

Bartolák-Suki, E., Imsirovic, J., Parameswaran, H., Wellman, T. J., Martinez, N., Allen, P. G., et al. (2015). Fluctuation-driven Mechanotransduction Regulates Mitochondrial-Network Structure and Function. *Nat. Mater.* 14, 1049–1057. doi:10.1038/nmat4358

Bartolák-Suki, E., and Suki, B. (2020). Tuning Mitochondrial Structure and Function to Criticality by Fluctuation-Driven Mechanotransduction. *Sci. Rep.* 10, 407. doi:10.1038/s41598-019-57301-1

Bastounis, E. E., Yeh, Y. T., and Theriot, J. A. (2019). Subendothelial Stiffness Alters Endothelial Cell Traction Force Generation while Exerting a Minimal Effect on the Transcriptome. *Sci. Rep.* 9, 18209. doi:10.1038/s41598-019-54336-2

Brangwynne, C. P., MacKintosh, F. C., Kumar, S., Geisse, N. A., Talbot, J., Mahadevan, L., et al. (2006). Microtubules Can bear Enhanced Compressive Loads in Living Cells Because of Lateral Reinforcement. *J. Cel Biol* 173, 733–741. doi:10.1083/jcb.200601060

Brown, X. Q., Bartolak-Suki, E., Williams, C., Walker, M. L., Weaver, V. M., and Wong, J. Y. (2010). Effect of Substrate Stiffness and PDGF on the Behavior of Vascular Smooth Muscle Cells: Implications for Atherosclerosis. *J. Cel Physiol* 225, 115–122. doi:10.1002/jcp.22202

Brozovich, F. V., Nicholson, C. J., Degen, C. V., Gao, Y. Z., Aggarwal, M., and Morgan, K. G. (2016). Mechanisms of Vascular Smooth Muscle Contraction and the Basis for Pharmacologic Treatment of Smooth Muscle Disorders. *Pharmacol. Rev.* 68, 476–532. doi:10.1124/pr.115.010652

Caliari, S. R., and Burdick, J. A. (2016). A Practical Guide to Hydrogels for Cell Culture. *Nat. Methods* 13, 405–414. doi:10.1038/nmeth.3839

Čermák, V., Dostál, V., Jelínek, M., Libusová, L., Kovář, J., Rösel, D., et al. (2020). Microtubule-targeting Agents and Their Impact on Cancer Treatment. *Eur. J. Cel Biol.* 99, 151075. doi:10.1016/j.ejcb.2020.151075

Clarke, M. C., Figg, N., Maguire, J. J., Davenport, A. P., Goddard, M., Littlewood, T. D., et al. (2006). Apoptosis of Vascular Smooth Muscle Cells Induces Features of Plaque Vulnerability in Atherosclerosis. *Nat. Med.* 12, 1075–1080. doi:10.1038/nm1459

Claudie, P., Alain, G., and Stéhane, A. (2019). Traction Force Measurements of Human Aortic Smooth Muscle Cells Reveal a Motor-Clutch Behavior. *Mol. Cell Biomech.* 16, 87–108. doi:10.32604/mcb.2019.06415

Colin-York, H., and Fritzsche, M. (2018). The Future of Traction Force Microscopy. *Curr. Opin. Biomed. Eng.* 5, 1–5. doi:10.1016/j.cobme.2017.10.002

Discher, D. E., Janmey, P., and Wang, Y. L. (2005). Tissue Cells Feel and Respond to the Stiffness of Their Substrate. *Science* 310, 1139–1143. doi:10.1126/science.1116995

Glasser, S. P., Arnett, D. K., McVeigh, G. E., Finkelstein, S. M., Bank, A. J., Morgan, D. J., et al. (1997). Vascular Compliance and Cardiovascular Disease: A Risk Factor or a Marker? *Am. J. Hypertens.* 10, 1175–1189. doi:10.1016/S0895-7061(97)00311-7

Haase, K., and Pelling, A. E. (2015). Investigating Cell Mechanics with Atomic Force Microscopy. *J. R. Soc. Interf.* 12, 20140970. doi:10.1098/rsif.2014.0970

Halaidych, O. V., Cochrane, A., van den Hil, F. E., Mummery, C. L., and Orlova, V. V. (2019). Quantitative Analysis of Intracellular Ca2+ Release and Contraction in hiPSC-Derived Vascular Smooth Muscle Cells. *Stem Cel Rep.* 12, 647–656. doi:10.1016/j.stemcr.2019.02.003

Holle, A. W., Young, J. L., Van Vliet, K. J., Kamm, R. D., Discher, D., Janmey, P., et al. (2018). Cell-Extracellular Matrix Mechanobiology: Forceful Tools and Emerging Needs for Basic and Translational Research. *Nano Lett.* 18, 1–8. doi:10.1021/acs.nanolett.7b04982

Johnson, R. T., Solanki, R., and Warren, D. T. (2021). Mechanical Programming of Arterial Smooth Muscle Cells in Health and Ageing. *Biophys. Rev.* 13, 757–768. doi:10.1007/s12551-021-00833-6

Joo, E. E., and Yamada, K. M. (2014). MYPT1 Regulates Contractility and Microtubule Acetylation to Modulate Integrin Adhesions and Matrix Assembly. *Nat. Commun.* 5, 3510. doi:10.1038/ncomms4510

Kandow, C. E., Georges, P. C., Janmey, P. A., and Beningo, K. A. (2007). "Polyacrylamide Hydrogels for Cell Mechanics: Steps toward Optimization and Alternative Uses," in *Methods in Cell Biology Cell Mechanics* (Academic Press), 29–46. doi:10.1016/S0091-679X(07)83002-0

Kraning-Rush, C. M., Carey, S. P., Califano, J. P., and Reinhart-King, C. A. (2012). "Quantifying Traction Stresses in Adherent Cells," in *Computational Methods in Cell Biology*. Editors A. R. Asthagiri and A. P. Arkin (Academic Press), 139–178. doi:10.1016/B978-0-12-388403-9.00006-0

Lacolley, P., Regnault, V., Segers, P., and Laurent, S. (2017). Vascular Smooth Muscle Cells and Arterial Stiffening: Relevance in Development, Aging, and Disease. *Physiol. Rev.* 97, 1555–1617. doi:10.1152/physrev.00003.2017

Leite, R., and Webb, R. C. (1998). Microtubule Disruption Potentiates Phenylephrine-Induced Vasoconstriction in Rat Mesenteric Arterial Bed. *Eur. J. Pharmacol.* 351, R1–R3. doi:10.1016/S0014-2999(98)00358-6

Lekka, M., Gnanachandran, K., Kubiak, A., Zieliński, T., and Zemła, J. (2021). Traction Force Microscopy - Measuring the Forces Exerted by Cells. *Micron* 150, 103138. doi:10.1016/j.micron.2021.103138

Li, S., Sims, S., Jiao, Y., Chow, L. H., and Pickering, J. G. (1999). Evidence from a Novel Human Cell Clone that Adult Vascular Smooth Muscle Cells Can Convert Reversibly between Noncontractile and Contractile Phenotypes. *Circ. Res.* 85, 338–348. doi:10.1161/01.res.85.4.338

Li, X., Ni, Q., He, X., Kong, J., Lim, S. M., Papoian, G. A., et al. (2020). Tensile Force-Induced Cytoskeletal Remodeling: Mechanics before Chemistry. *Plos Comput. Biol.* 16, e1007693. doi:10.1371/journal.pcbi.1007693

Liu, R., Leslie, K. L., and Martin, K. A. (2015). Epigenetic Regulation of Smooth Muscle Cell Plasticity. *Biochim. Biophys. Acta* 1849, 448–453. doi:10.1016/j.bbagrm.2014.06.004

Minaisah, R.-M., Cox, S., and Warren, D. T. (2016). "The Use of Polyacrylamide Hydrogels to Study the Effects of Matrix Stiffness on Nuclear Envelope Properties," in The Nuclear Envelope *Methods in Molecular Biology*. Editors S. Shackleton, P. Collas, and E. C. Schirmer (New York, NY: Springer New York), 233–239. doi:10.1007/978-1-4939-3530-7_15

Mitchell, G. F., Hwang, S. J., Vasan, R. S., Larson, M. G., Pencina, M. J., Hamburg, N. M., et al. (2010). Arterial Stiffness and Cardiovascular Events: the Framingham Heart Study. *Circulation* 121, 505–511. doi:10.1161/CIRCULATIONAHA.109.886655

Mohammed, D., Versaevel, M., Bruyère, C., Alaimo, L., Luciano, M., Vercruysse, E., et al. (2019). Innovative Tools for Mechanobiology: Unraveling Outside-In and Inside-Out Mechanotransduction. *Front. Bioeng. Biotechnol.* 7, 162. doi:10.3389/fbioe.2019.00162

Muhamed, I., Chowdhury, F., and Maruthamuthu, V. (2017). Biophysical Tools to Study Cellular Mechanotransduction. *Bioengineering (Basel)* 4, 12. doi:10.3390/bioengineering4010012

Nagayama, K., and Nishimiya, K. (2020). Moderate Substrate Stiffness Induces Vascular Smooth Muscle Cell Differentiation through Cellular Morphological and Tensional Changes. *Biomed. Mater. Eng.* 31, 157–167. doi:10.3233/BME-201087

Ngo, P., Ramalingam, P., Phillips, J. A., and Furuta, G. T. (2006). Collagen Gel Contraction Assay. *Methods Mol. Biol.* 341, 103–109. doi:10.1385/1-59745-113-4:103

Nogales, E. (2001). Structural Insight into Microtubule Function. *Annu. Rev. Biophys. Biomol. Struct.* 30, 397–420. doi:10.1146/annurev.biophys.30.1.397

Pasqualini, F. S., Agarwal, A., O'Connor, B. B., Liu, Q., Sheehy, S. P., and Parker, K. K. (2018). Traction Force Microscopy of Engineered Cardiac Tissues. *PLOS ONE* 13, e0194706. doi:10.1371/journal.pone.0194706

Pasquier, E., Honoré, S., and Braguer, D. (2006). Microtubule-targeting Agents in Angiogenesis: Where Do We Stand? *Drug Resist. Updat* 9, 74–86. doi:10.1016/j.drup.2006.04.003

Paul, R. J., Bowman, P. S., and Kolodney, M. S. (2000). Effects of Microtubule Disruption on Force, Velocity, Stiffness and [Ca(2+)](i) in Porcine Coronary Arteries. *Am. J. Physiol. Heart Circ. Physiol.* 279, H2493–H2501. doi:10.1152/ajpheart.2000.279.5.H2493

Platts, S. H., Falcone, J. C., Holton, W. T., Hill, M. A., and Meininger, G. A. (1999). Alteration of Microtubule Polymerization Modulates Arteriolar Vasomotor Tone. *Am. J. Physiol.* 277, H100–H106. doi:10.1152/ajpheart.1999.277.1.H100

Platts, S. H., Martinez-Lemus, L. A., and Meininger, G. A. (2002). Microtubule-Dependent Regulation of Vasomotor Tone Requires Rho-Kinase. *J. Vasc. Res.* 39, 173–182. doi:10.1159/000057765

Porter, L., Minaisah, R. M., Ahmed, S., Ali, S., Norton, R., Zhang, Q., et al. (2020). SUN1/2 Are Essential for RhoA/ROCK-Regulated Actomyosin Activity in Isolated Vascular Smooth Muscle Cells. *Cells* 9, 132. doi:10.3390/cells9010132

Qiu, H., Zhu, Y., Sun, Z., Trzeciakowski, J. P., Gansner, M., Depre, C., et al. (2010). Short Communication: Vascular Smooth Muscle Cell Stiffness as a Mechanism for Increased Aortic Stiffness with Aging. *Circ. Res.* 107, 615–619. doi:10.1161/CIRCRESAHA.110.221846

Ragnauth, C. D., Warren, D. T., Liu, Y., McNair, R., Tajsic, T., Figg, N., et al. (2010). Prelamin A Acts to Accelerate Smooth Muscle Cell Senescence and Is a Novel Biomarker of Human Vascular Aging. *Circulation* 121, 2200–2210. doi:10.1161/CIRCULATIONAHA.109.902056

Rensen, S. S., Doevendans, P. A., and van Eys, G. J. (2007). Regulation and Characteristics of Vascular Smooth Muscle Cell Phenotypic Diversity. *Neth. Heart J.* 15, 100–108. doi:10.1007/BF03085963

Rezvani-Sharif, A., Tafazzoli-Shadpour, M., and Avolio, A. (2019). Progressive Changes of Elastic Moduli of Arterial wall and Atherosclerotic Plaque Components during Plaque Development in Human Coronary Arteries. *Med. Biol. Eng. Comput.* 57, 731–740. doi:10.1007/s11517-018-1910-4

Rickel, A. P., Sanyour, H. J., Leyda, N. A., and Hong, Z. (2020). Extracellular Matrix Proteins and Substrate Stiffness Synergistically Regulate Vascular Smooth Muscle Cell Migration and Cortical Cytoskeleton Organization. *ACS Appl. Bio Mater.* 3, 2360–2369. doi:10.1021/acsabm.0c00100

Rzucidlo, E. M., Martin, K. A., and Powell, R. J. (2007). Regulation of Vascular Smooth Muscle Cell Differentiation. *J. Vasc. Surg.* 45 Suppl A, A25–A32. doi:10.1016/j.jvs.2007.03.001

Sanyour, H. J., Li, N., Rickel, A. P., Childs, J. D., Kinser, C. N., and Hong, Z. (2019). Membrane Cholesterol and Substrate Stiffness Co-ordinate to Induce the Remodelling of the Cytoskeleton and the Alteration in the Biomechanics of Vascular Smooth Muscle Cells. *Cardiovasc. Res.* 115, 1369–1380. doi:10.1093/cvr/cvy276

Sato, Y., Kamijo, K., Tsutsumi, M., Murakami, Y., and Takahashi, M. (2020). Nonmuscle Myosin IIA and IIB Differently Suppress Microtubule Growth to Stabilize Cell Morphology. *J. Biochem.* 167, 25–39. doi:10.1093/jb/mvz082

Sazonova, O. V., Isenberg, B. C., Herrmann, J., Lee, K. L., Purwada, A., Valentine, A. D., et al. (2015). Extracellular Matrix Presentation Modulates Vascular Smooth Muscle Cell Mechanotransduction. *Matrix Biol.* 41, 36–43. doi:10.1016/j.matbio.2014.11.001

Schierbaum, N., Rheinlaender, J., and Schäffer, T. E. (2019). Combined Atomic Force Microscopy (AFM) and Traction Force Microscopy (TFM) Reveals a Correlation between Viscoelastic Material Properties and Contractile Prestress of Living Cells. *Soft Matter* 15, 1721–1729. doi:10.1039/C8SM01585F

Schindelin, J., Arganda-Carreras, I., Frise, E., Kaynig, V., Longair, M., Pietzsch, T., et al. (2012). Fiji: an Open-Source Platform for Biological-Image Analysis. *Nat. Methods* 9, 676–682. doi:10.1038/nmeth.2019

Seetharaman, S., and Etienne-Manneville, S. (2020). Cytoskeletal Crosstalk in Cell Migration. *Trends Cel Biol* 30, 720–735. doi:10.1016/j.tcb.2020.06.004

Seetharaman, S., Vianay, B., Roca, V., Farrugia, A. J., De Pascalis, C., Boëda, B., et al. (2021). Microtubules Tune Mechanosensitive Cell Responses. *Nat. Mater.* 8, 1–12. doi:10.1038/s41563-021-01108-x

Sheridan, B. C., McIntyre, R. C., Meldrum, D. R., Cleveland, J. C., Agrafojo, J., Banerjee, A., et al. (1996). Microtubules Regulate Pulmonary Vascular Smooth Muscle Contraction. *J. Surg. Res.* 62, 284–287. doi:10.1006/jsre.1996.0209

Shi, N., and Chen, S. Y. (2016). Smooth Muscle Cell Differentiation: Model Systems, Regulatory Mechanisms, and Vascular Diseases. *J. Cel Physiol* 231, 777–787. doi:10.1002/jcp.25208

Stamenović, D. (2005). Microtubules May Harden or Soften Cells, Depending on the Extent of Cell Distension. *J. Biomech.* 38, 1728–1732. doi:10.1016/j.jbiomech.2004.07.016

Sun, Z., Martinez-Lemus, L. A., Hill, M. A., and Meininger, G. A. (2008). Extracellular Matrix-specific Focal Adhesions in Vascular Smooth Muscle Produce Mechanically Active Adhesion Sites. *Am. J. Physiol. Cel Physiol* 295, C268–C278. doi:10.1152/ajpcell.00516.2007

Thomopoulou, P., Sachs, J., Teusch, N., Mariappan, A., Gopalakrishnan, J., and Schmalz, H. G. (2016). New Colchicine-Derived Triazoles and Their Influence on Cytotoxicity and Microtubule Morphology. *ACS Med. Chem. Lett.* 7, 188–191. doi:10.1021/acsmedchemlett.5b00418

Tracqui, P., Broisat, A., Toczek, J., Mesnier, N., Ohayon, J., and Riou, L. (2011). Mapping Elasticity Moduli of Atherosclerotic Plaque *In Situ* via Atomic Force Microscopy. *J. Struct. Biol.* 174, 115–123. doi:10.1016/j.jsb.2011.01.010

Tsamis, A., Krawiec, J. T., and Vorp, D. A. (2013). Elastin and Collagen Fibre Microstructure of the Human Aorta in Ageing and Disease: a Review. *J. R. Soc. Interf.* 10, 20121004. doi:10.1098/rsif.2012.1004

Tseng, Q., Duchemin-Pelletier, E., Deshiere, A., Balland, M., Guillou, H., Filhol, O., et al. (2012). Spatial Organization of the Extracellular Matrix Regulates Cell-Cell junction Positioning. *Proc. Natl. Acad. Sci. U S A* 109, 1506–1511. doi:10.1073/pnas.1106377109

Vernon, R. B., and Gooden, M. D. (2002). An Improved Method for the Collagen Gel Contraction Assay. In Vitro *Cel Dev Biol Anim* 38, 97–101. doi:10.1290/1071-2690(2002)038<0097:AIMFTC>2.0.CO;2

Wang, L., Qiu, P., Jiao, J., Hirai, H., Xiong, W., Zhang, J., et al. (2017). Yes-Associated Protein Inhibits Transcription of Myocardin and Attenuates Differentiation of Vascular Smooth Muscle Cell from Cardiovascular Progenitor Cell Lineage. *Stem Cells* 35, 351–361. doi:10.1002/stem.2484

Warren, D. T., Tajsic, T., Porter, L. J., Minaisah, R. M., Cobb, A., Jacob, A., et al. (2015). Nesprin-2-dependent ERK1/2 Compartmentalisation Regulates the DNA Damage Response in Vascular Smooth Muscle Cell Ageing. *Cell Death Differ* 22, 1540–1550. doi:10.1038/cdd.2015.12

Wong, J. Y., Velasco, A., Rajagopalan, P., and Pham, Q. (2003). Directed Movement of Vascular Smooth Muscle Cells on Gradient-Compliant Hydrogels. *Langmuir* 19, 1908–1913. doi:10.1021/la026403p

Wu, S. Z., and Bezanilla, M. (2018). Actin and Microtubule Cross Talk Mediates Persistent Polarized Growth. *J. Cel Biol* 217, 3531–3544. doi:10.1083/jcb. 201802039

Xie, S. A., Zhang, T., Wang, J., Zhao, F., Zhang, Y. P., Yao, W. J., et al. (2018). Matrix Stiffness Determines the Phenotype of Vascular Smooth Muscle Cell *In Vitro* and *In Vivo*: Role of DNA Methyltransferase 1. *Biomaterials* 155, 203–216. doi:10.1016/j.biomaterials.2017.11.033

Ye, G. J., Nesmith, A. P., and Parker, K. K. (2014). The Role of Mechanotransduction on Vascular Smooth Muscle Myocytes' [corrected] Cytoskeleton and Contractile Function. *Anat. Rec. (Hoboken)* 297, 1758–1769. doi:10.1002/ar.22983

Zhang, D., Jin, N., Rhoades, R. A., Yancey, K. W., and Swartz, D. R. (2000). Influence of Microtubules on Vascular Smooth Muscle Contraction. *J. Muscle Res. Cel Motil* 21, 293–300. doi:10.1023/A: 1005600118157

Zhou, D. W., Lee, T. T., Weng, S., Fu, J., and García, A. J. (2017). Effects of Substrate Stiffness and Actomyosin Contractility on Coupling between Force Transmission and Vinculin-Paxillin Recruitment at Single Focal Adhesions. *Mol. Biol. Cel* 28, 1901–1911. doi:10.1091/mbc.e17-02-0116